

# Identification of the pore size distribution of a porous medium by yield stress fluids using Herschel-Bulkley model

A. OUKHLEF<sup>a</sup>, A. AMBARI<sup>b</sup>, S. CHAMPMARTIN<sup>b</sup>

a. USMS, LITA, École Supérieure de Technologie, BP : 591, 23000 Béni Mellal, Maroc,  
a.oukhlef.est@usms.ma

b. Arts et Métiers ParisTech, 2 bd du Ronceray, 49035 Angers, France,  
abdelhak.ambari@ensam.eu / stephane.champmartin@ensam.eu

## Résumé :

*Ce papier présente une nouvelle méthode qui permet de déterminer la distribution de tailles de pores (DTP) d'un milieu poreux. Cette technique innovante utilise les propriétés rhéologiques des fluides non newtoniens à seuil s'écoulant à travers l'échantillon poreux. Dans une première approche, le modèle de faisceaux de tubes capillaires sera utilisé. Par une simple mesure du débit total de fluide en fonction du gradient de pression imposé, il est possible de déterminer la DTP. En utilisant un fluide à seuil, le traitement mathématique des données expérimentales permet de donner un aperçu sur la répartition de tailles de pores du matériau poreux étudié. La technique proposée a été testée avec succès analytiquement et numériquement pour différentes distributions de tailles de pores classiques de type gaussien unimodal ou multimodal. L'étude a été appliquée aux fluides idéals à seuil de type Bingham et Casson. Cette étude a été étendue avec succès aux fluides réels de type Herschel-Bulkley. Contrairement aux autres méthodes complexes, onéreuses et parfois toxiques, elle présente plus d'avantages, engendre moins de coûts et nécessite une simple mesure, facile à interpréter. Cette nouvelle méthode pourrait ainsi devenir à l'avenir une méthode alternative, non toxique et peu coûteuse pour la caractérisation des matériaux poreux. Dans cette communication nous allons présenter l'aspect numérique de cette méthode afin d'identifier la DTP par l'utilisation des fluides viscoplastiques de type Herschel-Bulkley.*

## Abstract :

*In this paper, we present a new method that allows to determine the pore size distribution (PSD) in a porous medium. This innovative technique uses the rheological properties of non-Newtonian yield stress fluids flowing through the porous sample. In a first approach, the capillary bundle model will be used. The PSD can be possible to obtained from the measurement of the total flow rate of fluid as a function of the imposed pressure gradient. Using a yield stress fluid, the mathematical processing of experimental data provides to give an overview into the distribution of the pore size in the porous material. The technique proposed was successfully tested analytically and numerically for usual pore size distributions such as the Gaussian mono and multimodal distributions. The study was applied to the ideals yield stress fluids Bingham and Casson. This study was successfully extended to real fluids of*

*Herschel-Bulkley model. Unlike other complex methods, expensive and sometimes toxic, this technique has more advantages, creates a lower costs, requires simple measurement and easy to interpret. This new method could become in the future an alternative, non-toxic and cheap method for the characterization of porous materials. In this paper we will present the numerical aspect of this method in order to identify the PSD by non-Newtonian viscoplastic fluids using Herschel-Bulkley model.*

**Keywords : Porous materials, Pore-size distribution, Non-Newtonian yield stress fluids, Herschel-Bulkley model**

## 1 Introduction

Porous media are found almost everywhere around us [1, 2, 3, 4], whether in living matter (human skin, cartilage, bone ...), inert (soils, layers sedimentary rocks ...) or industrial (concretes, cements, powders, textiles ...). The characterization of porous media in terms of porosity, specific surface and PSD etc, is an important issue for many industrial sectors : assisted recovery petroleum, thermal building,  $CO_2$  sequestration, energy storage ... So, the Phenomenon of transports related to the flows through the porous media have occupied and continue to stimulate a strong research activity as fundamental applied. The main objective of this work is to propose a new method non-polluting, simple and economic, unlike other existing currently processes.

Indeed, among the experimental methods most used to characterize porous media in terms of PSD, we can cite traditional methods such as : (i) the mercury intrusion porosimetry (MIP) [1, 2, 3, 5]. This technique is based on the existence of a threshold below which the pores cannot be invaded. Indeed due to its large surface tension mercury does not wet most of the materials. A pressure difference  $\Delta P_{lg}$  must be imposed so that mercury penetrates the pores whose radii  $r_p$  are greater than  $r_p^* = 2\sigma_{lg} \cos \theta / \Delta P_{lg}$  where  $\sigma_{lg}$  is the liquid/gas interfacial tension and  $\theta$  the contact angle. Because of the harmful effects of mercury vapor, this technique is destined to be abandoned, (ii) the method of isothermal adsorption [6] due the molecular Van der Waals interactions between a condensing vapor and the internal surface of the pores. There are other alternative techniques that can characterize the PSD. However, they are more difficult to implement and also expensive : the thermoporometry [7], the Small Angle Neutron (SANS) or X-Ray Scattering (SAXS) [8, 9], nuclear magnetic resonance (NMR) [10] ... Other destructive methods, such as stereology [11].

These two classical methods use the existence of a threshold below which the pores can't be invaded according to a thermodynamic parameter of control. Like the aforementioned techniques, our new approach is based on the injection of non-Newtonian yield stress fluid of Herschel-Bulkley model into the porous medium (invasive method). The spirit of the suggested method is to use the rheological properties of yield stress effect to scan different pore scales to determine its PSD. The basic idea is the following : in order to set such fluids into motion, it is necessary to impose between both ends of a pore a pressure gradient ( $\nabla P$ ) greater than a critical value depending on the fluid yield stress ( $\tau_0$ ) and the pore radius ( $r_p$ ). In other words, for the pressure gradient  $\nabla P$ , only the pores whose radius is greater than the critical radius  $r_0 = 2\tau_0 / \nabla P$  are invaded. Then it is possible to scan the PSD by increasing the pressure gradient step by step and measuring the corresponding flow rate  $Q$ . So, This work consists in solving the inverse problem which is reduced to the determination of the PSD of a porous medium, by the simple measurement of the volume flow rate evolution of a non-Newtonian yield stress fluid (Herschel-Bulkley

model) which crosses it, according to the pressure gradient imposed on it :  $Q = f(\nabla P)$ . This technique has been successfully tested on unimodal, bi or tri-modal Gaussian distributions. Firstly, by using ideal fluids such as Bingham and Casson [12]. Secondly, since it is difficult to find fluids of this type, we have generalized this method to more complex viscoplastic fluids such as Herschel-Bulkley fluids [13], which better describe most of the non-Newtonian yield stress fluids. In this work, we will give the results of this generalized model by presenting in this part the analytical expression of the solution of the inverse problem coming from the resolution of the associated integral equation described below. So we can calculate the probability density depending on the partial derivatives (integer or fractional) of the characteristic curve ( $Q = f(\nabla P)$ ).

Finally, we have been able by this work to improve this technique : the problem inverse solution of the PSD identification using method based on a numerical approach with yield stress fluids such as Herschel-Bulkley model.

## 2 Models and procedure

### 2.1 Formulation of the problem and solution

The porous materials can be described by a capillary bundle model [14, 15], the radii of which are distributed according to a probability density function  $p(r)$ . This model, originally introduced by Purcell [16], continues to be used in many studies of porous media. This pore construction, which does not take into account the tortuosity, the interconnectivity, the permeability and the variation in the pore cross-section along a pore traversed by the fluid, is only apparently criticizable because corrections taking into account these parameters can be introduced later to correct this modeling. In our study we ignore the tortuosity that only affects the characteristic curve by increasing the length of the pores [1, 2] and not the non-dimensional PSD. Nevertheless the interconnectivity cannot be modeled. We will use this model to derive the inversion technique which allows us to obtain the PSD from the characteristic curve for a given yield stress fluid in non-inertial regimes. Under these conditions, the expression of the total flow rate through this capillary model, when a pressure gradient  $\nabla P$  is imposed on this system, as a function of the elementary flow rate  $q(\nabla P, r)$  in each capillary, and of the probability density  $p(r)$  constitutes a Volterra equation of the first kind.

$$Q(\nabla P) = \int_{r_0 = \frac{2\tau_0}{\nabla P}}^{\infty} q(\nabla P, r) p(r) dr \quad (1)$$

We want to identify the probability density  $p(r)$  from the curve describing the evolution of total flow  $Q(\nabla P)$  as a function of the pressure gradient of a Herschel-Bulkley fluid (H-B) through a porous medium. This measured flow is calculated directly from the integral Eq. (1) when  $p(r)$  is known. If this distribution is unknown, this relation constitutes a Volterra equation of the first kind, with the kernel  $q(\nabla P, r)$  is the elementary flow of each capillary, previously calculated, and  $Q(\nabla P)$  constitutes the source term obtained experimentally. Indeed, the Herschel-Bulkley model is used because it describes the rheological behavior of most non-Newtonian yield stress fluids more realistically than the Bingham model. It is, in fact, a generalization of the last model which takes into account the pseudoplastic or dilatant behavior of the real yield stress fluids. In this model, beyond the yield stress  $\tau_0$ , the linearity of the shear rate has been replaced by a power law behavior. It is therefore a model with three parameters : the yield stress  $\tau_0$ , the consistency of the fluid  $k$  and power-law index  $n$ . The rheological behavior law

describing this model is given by :

$$\begin{cases} \underline{\underline{\tau}} = 2 \left( k \left( \sqrt{2\underline{\underline{D}} : \underline{\underline{D}}} \right)^{n-1} + \frac{\tau_0}{\sqrt{2\underline{\underline{D}} : \underline{\underline{D}}}} \right) \underline{\underline{D}} & \text{for } \sqrt{\frac{\underline{\underline{\tau}} : \underline{\underline{\tau}}}{2}} > \tau_0 \\ \underline{\underline{D}} = 0 & \text{for } \sqrt{\frac{\underline{\underline{\tau}} : \underline{\underline{\tau}}}{2}} \leq \tau_0 \end{cases} \quad (2)$$

with  $\underline{\underline{\tau}}$  the shear stress tensor and  $\underline{\underline{D}}$  the rate of deformation tensor. For the flow in a tube with circular cross-section, these equations take the simpler form :

$$\begin{cases} \tau_{r'z} = \tau_0 + k \left| \frac{\partial u_z}{\partial r'} \right|^n & \text{for } \tau_{r'z} > \tau_0 \\ \frac{\partial u_z}{\partial r'} = 0 & \text{for } \tau_{r'z} \leq \tau_0 \end{cases} \quad (3)$$

where  $\tau_{r'z}$  is the shear stress,  $(\partial u_z / \partial r')$  the rate of deformation and  $r'$  is the radial coordinate.

The elementary flow rate of the Herschel-Bulkley fluid through a capillary of circular cross-section which constitutes the kernel of Eq. (1) is given by [17] :

$$q(\nabla P, r, n) = \begin{cases} n\pi r^3 \left( \frac{r\nabla P}{2k} \right)^{\frac{1}{n}} \left( 1 - \frac{r_0}{r} \right)^{(n+1)/n} \\ \left[ \frac{\left( 1 - \frac{r_0}{r} \right)^2}{(3n+1)} + \frac{2r_0}{r} \frac{\left( 1 - \frac{r_0}{r} \right)}{(2n+1)} + \frac{\left( \frac{r_0}{r} \right)^2}{(n+1)} \right] & \text{for } r > r_0 \\ 0 & \text{for } r \leq r_0 \end{cases} \quad (4)$$

For  $r \leq r_0$  the fluid does not flow. The critical radius  $r_0 = 2\tau_0 / \nabla P$  is also the radius of the core zone of the plug flow.

The pore size distribution  $p(r)$  can be obtained through differential operators applied to  $Q(\nabla P)$  [13] :

$$p(r) = \frac{2^{(1+3n)/n} k^{1/n} (\nabla P)^2}{16 ((1/n)!) \pi \tau_0 r^{(1+3n)/n}} \left[ \left( \frac{1+4n}{n} \right) \frac{\partial^{(1+n)/n}}{\partial (\nabla P)^{(1+n)/n}} + \nabla P \frac{\partial^{(1+2n)/n}}{\partial (\nabla P)^{(1+2n)/n}} \right] Q \Big|_{\nabla P = \frac{2\tau_0}{r}} \quad (5)$$

It should be noted that for  $n = 1$  the Herschel-Bulkley model it is reduced to that of Bingham fluid and the Eq. (5) is reduced to that obtained by Ambari et al. [18].

## 2.2 Analytical inverse method for determining PSD

In the case where the power-law index is  $n = 1/q$  with  $q \in \mathbb{N}^*$ , a general relationship is obtained between the probability density  $p(r)$  and the integer partial derivatives of the total flow  $\partial^i Q / \partial (\nabla P)^i$ . In the case where  $n$  is non-integer it is possible to generalize this formula considering these derivatives as fractional. This will be justified later. In order to reduce the number of physical parameters involved in this problem, we will normalize the previous equations, using as characteristic length and pressure

gradient  $L$  and  $\tau_0/L$  where  $r^+ = r/L$  and  $(\nabla P)^+ = \nabla P / (\tau_0/L)$ . Note that  $L$  is taken here equal to the thickness of the studied sample (directly measurable) and not the mean radius of the capillaries which is still unknown and requires a complementary measurement. Therefore, the non-dimensional kernel is then given by :

$$q^+((\nabla P)^+, r^+, n) = \begin{cases} He^{H-B} \frac{1}{2^{1/n}} \frac{1}{(2n+1)} \frac{1}{((\nabla P)^+)^3} (r^+ (\nabla P)^+ - 2)^{(1+1/n)} \\ \quad [8n^2 + 4n(n+1)r^+(\nabla P)^+ + \\ \quad (n(2n+3)+1)(r^+)^2((\nabla P)^+)^2] \text{ for } r^+ > r_0^+ \\ 0 \text{ for } r^+ \leq r_0^+ \end{cases} \quad (6)$$

With  $He^{H-B} = \rho \tau_0^{(2-n)/n} L^2 / k^{(2/n)}$  is the Hedström number in the case of a Herschel Bulkley fluid [19],  $\rho$  the density of fluid and  $r_0^+ = 2 / (\nabla P)^+$  the non-dimensional critical radius. The characteristic flow is then defined by :

$$q_c = \frac{n\pi}{(3n+1)(n+1)} \left( \frac{Lk^{1/n}\tau_0^{(n-1)/n}}{\rho} \right) \quad (7)$$

Fig. 1 below, presents the evolution of the elementary flow rate in a radius pore  $r^+ = 1$  as a function of the imposed pressure gradient  $(\nabla P)^+$  (that is to say the kernel), for different power-law index but for a number of Hedström  $He^{H-B} = 0.02$ .

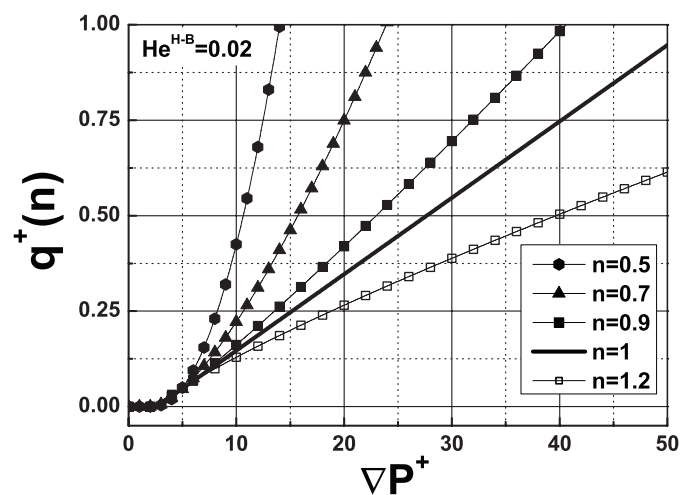


FIGURE 1: Elementary flow vs. pressure gradient for different power-law index and  $He^{H-B} = 0.02$ .

As for non-dimensional pore size distribution :

$$p^+(r^+) = \frac{n ((\nabla P)^+)^{(1+5n)/n}}{16(1+3n)(1+n)((1/n)!)} He^{H-B} \left[ \left( \frac{1+4n}{n} \right) \frac{\partial^{(1+n)/n}}{\partial ((\nabla P)^+)^{(1+n)/n}} + (\nabla P)^+ \frac{\partial^{(1+2n)/n}}{\partial ((\nabla P)^+)^{(1+2n)/n}} \right] Q^+ \Big|_{(\nabla P)^+ = \frac{2}{r^+}} \quad (8)$$

In the case, where  $n$  is non-integer, the calculation of the fractional derivatives which intervene in the previous relation (Eq. 8) that makes it possible to calculate the inverse distribution, is carried out by means of the following relation defined by Riemann [20] :

$$\frac{d^\nu (x^m)}{dx^\nu} = \frac{\Gamma(m+1)}{\Gamma(m-\nu+1)} x^{m-\nu} \quad (9)$$

Where  $\nu$  is the non-integer derivation order,  $\Gamma$  the Gamma function and  $m$  the order of the derivative of a monomial, with  $(x = \nabla P)$ . In our study, the above relation will be used to calculate the different fractional derivatives that occur in each case treated, after a polynomial fit of the evolution  $Q = f(\nabla P)$  (see Eq. 1).

Therefore, we will try to identify the inverse distribution to compare it with the one imposed initially. For this, we have fitted the 1000 points of the direct characteristic by a polynomial function of order 40 to carry out the interpolations necessary for the calculations. Subsequently we proceeded to the calculation of the fractional derivatives (remember that in the case where  $n = 1/q$  with  $q \in \mathbb{N}^*$ , the two successive derivatives are integers). In all cases, the distribution will be calculated by using equation 8. In what follows, we will explain the approach followed to obtain this inverse distribution.

### 2.2.1 Inversion in the case of a Bingham fluid (n=1)

Previously we assume that the distribution is of Gaussian type, normalized using  $L$  as the characteristic length,  $\mu^+ = \mu/L$  and  $\sigma^+ = \sigma/L$ , where  $\mu$  is the mean value and standard deviation  $\sigma$ . we will write from now on the equations in non-dimensional form :

$$p^+(r^+) = \frac{1}{\sigma^+ \sqrt{2\pi}} \exp \left[ -\frac{(r^+ - \mu^+)^2}{2\sigma^{+2}} \right] \quad (10)$$

Now, it is possible to normalize the Volterra equation (Eq. 1) as follows :

$$Q^+(\nabla P^+) = \int_{r_0^+ = \frac{2}{\nabla P^+}}^{\infty} q^+(\nabla P^+, r^+, n) p^+(r^+) dr^+ \quad (11)$$

Its evolution is represented by the characteristic curve below (Fig. 2) for  $\mu^+ = 10^{-4}$ ,  $\sigma^+ = 2.10^{-5}$  and  $He^{H-B} = 0.02$ . This figure shows the non-dimensional total flow rate vs. the non-dimensional pressure gradient resulting from the flow of the Bingham fluid through such a porous medium. This flow rate is calculated by Eq. 11. This figure is characterized by a first region at low pressure gradients in which the flow rate is zero. This region extends until the largest pore in the material is invaded. It is followed by

a second region in which the flow rate increases with the pressure gradient. In a second step, the given distribution is forgotten and the flow rate vs. pressure gradient (or the characteristic curve) given by the initial calculation (or obtained by an experiment) is used as a starting point. It should be noted that for  $n = 1$  the identification relation of the PSD is given by :

$$p^+(r^+) = \frac{(\nabla P^+)^6}{128He^{H-B}} \left[ 5 \frac{\partial^2}{\partial (\nabla P^+)^2} + \nabla P^+ \frac{\partial^3}{\partial (\nabla P^+)^3} \right] Q^+ \Big|_{\nabla P^+ = \frac{2}{r^+}} \quad (12)$$

Now, Eq. 12 is applied to the non-dimensional characteristic curve (Fig. 2) to calculate  $p^+(r^+)$  which is plotted in Fig. 3(a). This figure exhibits a perfect agreement between the original Gaussian distribution and the one calculated with the relationship obtained for  $p^+(r^+)$  by the inverse method (see the article [12]).

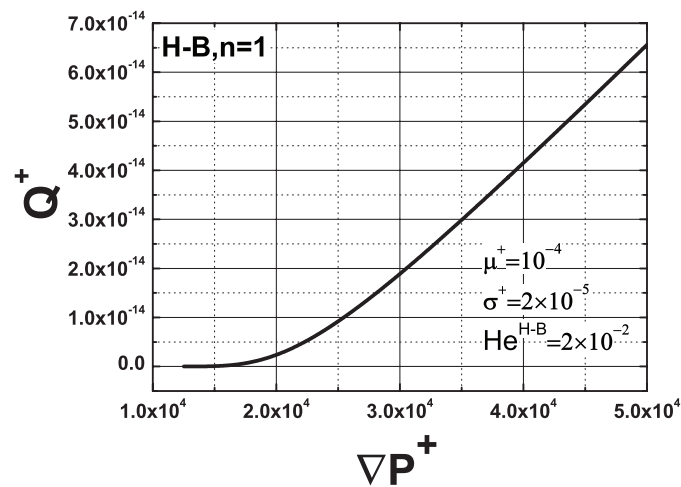


FIGURE 2: Total flow rate vs. pressure gradient for a Gaussian distribution and a Bingham fluid for  $He^{H-B} = 0.02$ .

In this case, although the identification relation of the pore size distribution (Eq. 12) includes integer derivatives, to determine  $p^+(r^+)$  we carried out calculations with the technique using fractional derivatives and a fit of the 1000 points of the characteristic curve (Fig. 2). The results obtained by this method are shown in figure 3(b). They show that this technique is applicable, but introduces noise (small radii) related to the polynomial fit needed here. Indeed, if we use this same fit with the analytical method we find this noise.

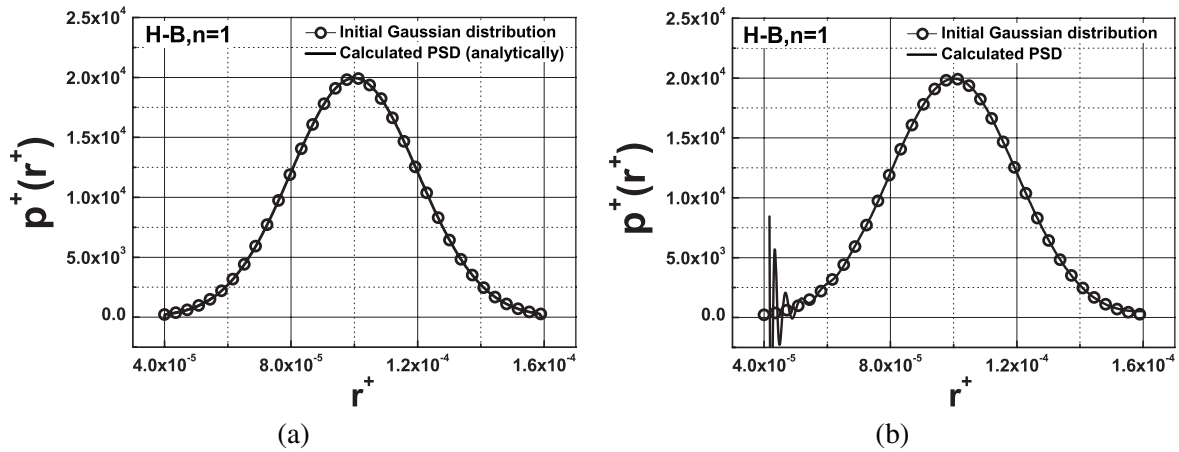


FIGURE 3: (a) Comparison between the initial and the analytical calculated PSD for a Bingham fluid (b) Comparison between the initial and the fractional method calculated PSD for a Bingham fluid.

**2.2.2 Inversion in the case of a Herschel-Bulkley fluid for  $n=1/q$  with  $q \in \mathbb{N}^*$**

As in all cases where  $n = 1/q$  with  $q \in \mathbb{N}^*$ , the expression of the inversion only depends on the integer derivatives :  $1 + q$  and  $2 + q$ . For example, when the power-law index  $n = 1/2$ , we get :

$$p^+(r^+) = \frac{(\nabla P^+)^7}{240He^{H-B}} \left[ 6 \frac{\partial^3}{\partial (\nabla P^+)^3} + \nabla P^+ \frac{\partial^4}{\partial (\nabla P^+)^4} \right] Q^+ \Big|_{\nabla P^+ = \frac{2}{r^+}} \quad (13)$$

Similarly to the previous section 2.2.1, when the PSD is supposed to be the same Gaussian distribution as the one used in this section, the calculated total flow rate is shown in Fig. 4.

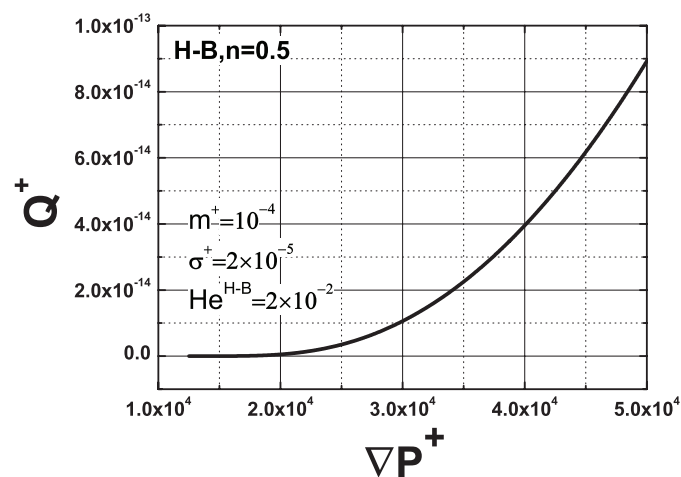


FIGURE 4: Total flow rate vs. pressure gradient for a Gaussian distribution and a Herschel-Bulkley fluid ( $n = 1/2$ ) for  $He^{H-B} = 0.02$ .

Now, when Eq. 13 is applied to the characteristic curve (Fig. 4), the initially injected Gaussian PSD is retrieved as we can see in Fig. 5(a). Also, This distribution can be obtained by using the fractional derivatives method (Fig. 5(b)), we can also obtain a perfect identification of the pore size distribution to the fluctuations introduced by the fit.



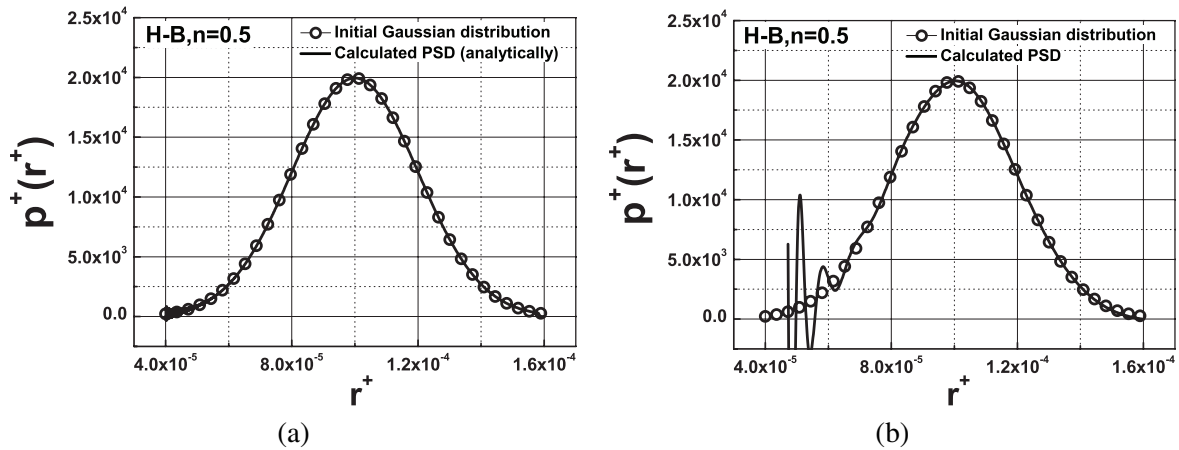


FIGURE 5: (a) Comparison between the initial and the analytical calculated PSD for a Herschel-Bulkley fluid with  $n = 0.5$  (b) Comparison between the initial and the fractional method calculated PSD for a Herschel-Bulkley fluid with  $n = 0.5$ .

### 2.2.3 Inversion in the case of a Herschel-Bulkley fluid for $n \in \mathbb{Q}$

In the case where the fluid has the pseudoplastic or shear-thinning behavior with  $n$  non-integer, for example  $n = 0.9$  and  $n = 1.2$ , the identification formula (Eq. 8) now intervenes non-integer derivatives. In this case, using only the fractional inversion method described above, from a fit of the 1000 points of the characteristic curve by a polynomial function of order 40, we obtain the results below (Fig. 6(b) and Fig. 7(b)) :

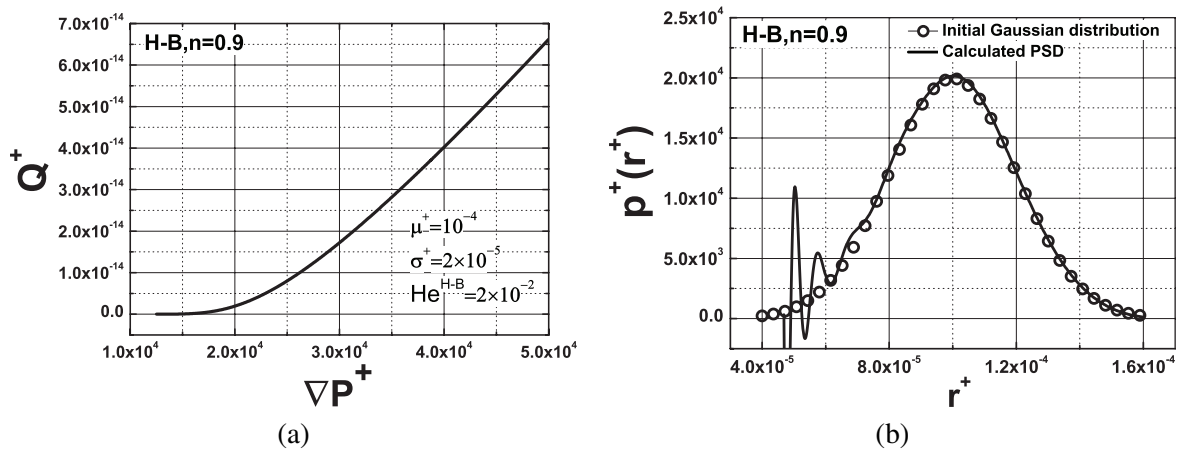


FIGURE 6: (a) Total flow rate vs. pressure gradient for a Gaussian distribution and a Herschel-Bulkley fluid with  $n = 0.9$  (b) Comparison between the initial and the fractional method calculated PSD for a Herschel-Bulkley fluid with  $n = 0.9$ .

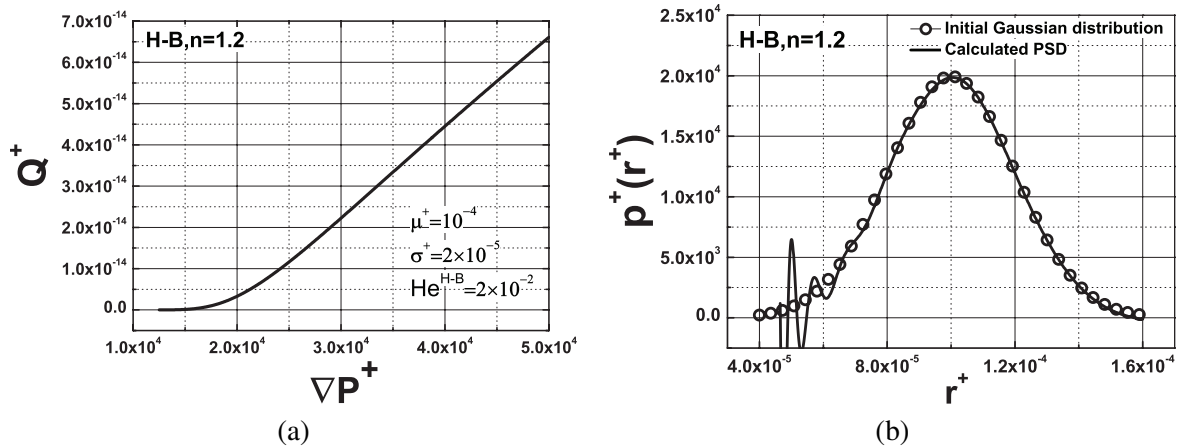


FIGURE 7: (a) Total flow rate vs. pressure gradient for a Gaussian distribution and a Herschel-Bulkley fluid with  $n = 1.2$  (b) Comparison between the initial and the fractional method calculated PSD for a Herschel-Bulkley fluid with  $n = 1.2$ .

From these two results (Fig. 6(b) and Fig. 7(b)), we note that the inverse distribution can be perfectly obtained by the method using the fractional derivatives with the fluctuations introduced by the precision of the type of fit used. Therefore, we will present in the next section another numerical method effective and robust and can be applied to all yield stress fluids such as the Herschel–Bulkley fluids and for all kinds of distributions.

### 2.3 Numerical inverse method for determining PSD

To solve the Volterra equation (Eq. 1), we can use a matrix resolution method in preference to the use of the successive derivative method, which leads to analytical identification relations requiring the use of fractional derivatives, in the case where the power-law index of the fluid is not of the form where  $n = 1/q$  with  $q \in \mathbb{N}^*$ . For this, we adopt the following approach : we discretize the source function as a function of the pressure gradient from 1 to  $N$  and we note  $Q_j(n) = Q_j(\nabla P_j, n)$  that the kernel is doubly discretized from 1 to  $N$  for  $i$  and  $j$ , so,  $q_{ij}(n) = q(\nabla P_j, r_i, n)$  (this constitutes the matrix to be inverted) as for the density of probability it is discretized as a function of the radius  $p_i = p(r_i)$ .

The Volterra equation is then rewritten as follows :

$$Q_j(n) = \sum_{i=1}^N q(\nabla P_j, r_i, n) p(r_i) \Delta r \quad \text{for} \quad j = 1, \dots, N \quad (14)$$

or in matrix form with :  $\Delta r = (r_{max} - r_{min})/(N - 1)$

$$\underline{Q} = (\underline{q} \cdot \underline{p}) \Delta r \quad (15)$$

Mathematically, if the kernel  $\underline{q}$  is not singular, a unique solution exists and is given by the following relation, where  $\underline{q}^{-1}$  is the inverse matrix of  $\underline{q}$  :

$$\underline{p} = \frac{1}{\Delta r} (\underline{q}^{-1} \cdot \underline{Q}) \quad (16)$$

### 2.3.1 Numerical approach

In the conditions of a Herschel-Bulkley type yield stress fluid, the conditions of the flow must be taken into account. For this we use the kernel in the non-dimensional form written in Eq. 6. This kernel is discretized on the basis of the radii and pressure gradients.

Where :

$$i, j = 1, \dots, N, \Delta r^+ = (r_{max}^+ - r_{min}^+) / (N - 1)$$

and

$$\Delta(\nabla P)^+ = ((\nabla P)_{max}^+ - (\nabla P)_{min}^+) / (N - 1)$$

with :

$$(\nabla P)_{min}^+ = 2/r_{max}^+ \text{ and } (\nabla P)_{max}^+ = 2/r_{min}^+$$

with  $r_{min}^+$  and  $r_{max}^+$  are previously fixed. Then :

$$r_i^+ = r_{min}^+ + (i - 1) \Delta r^+ \text{ and } (\nabla P)_j^+ = (\nabla P)_{min}^+ + (j - 1) \Delta(\nabla P)^+$$

The kernel matrix is then built with previously discretized elements.

$$\underline{\underline{q}}^+(n) = \begin{pmatrix} q^+((\nabla P)_{min}^+, r_{min}^+, n) & \dots & q^+((\nabla P)_{min}^+, r_{min}^+ + (i-1)\Delta r^+, n) & \dots & q^+((\nabla P)_{min}^+, r_{max}^+, n) \\ \vdots & \vdots & \vdots & \vdots & \vdots \\ q^+((\nabla P)_j^+, r_{min}^+, n) & \vdots & \ddots & \vdots & q^+((\nabla P)_j^+, r_{max}^+, n) \\ \vdots & \vdots & \vdots & \vdots & \vdots \\ q^+((\nabla P)_{max}^+, r_{min}^+, n) & \dots & q^+((\nabla P)_{max}^+, r_{min}^+ + (i-1)\Delta r^+, n) & \dots & q^+((\nabla P)_{max}^+, r_{max}^+, n) \end{pmatrix} \quad (17)$$

At this point, after having experimentally obtained the  $N$  components of the source vector  $\underline{Q}$  and calculated the inverse of the kernel matrix  $\underline{\underline{q}}^{-1}$ , we can determine unknown distribution  $\underline{p}$  (in our case it was assumed then totally forgotten in a second time). The number of values used (here  $N = 1000$ ) can naturally be very small depending on the desired accuracy. Indeed, to numerically invert the Volterra equation, we no longer need a large number of values as required by the computation of high order derivatives in previous methods.

### 2.3.2 Numerical inversions of some distributions by using Herschel-Bulkley model

#### — Herschel-Bulkley fluid (with $n = 1$ ; Bingham model)

As in most experiments it is difficult to have a large number  $N$  of points, we have verified with success on figure 8(b) that the precision of these computations is not very affected if we content ourselves with  $N = 25$  points instead of 1000 points.

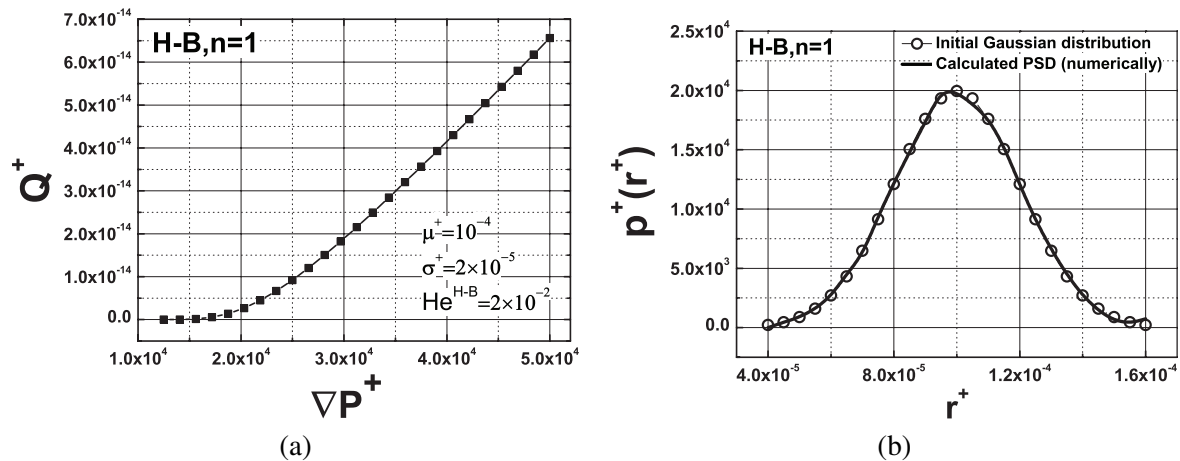


FIGURE 8: (a) Total flow rate vs. pressure gradient for a Gaussian distribution and a Bingham fluid ( $N = 25$ ) (b) Comparison between the initial and the numerical method calculated PSD for a Bingham model with ( $N = 25$ ).

To verify the efficiency of this numerical technique with more complex distributions, a bimodal Gaussian distribution is considered, with two peaks at  $\mu_1^+ = \mu_1/L$  and  $\mu_2^+ = 2\mu_1^+$  and different standard deviations  $\sigma_2^+ = 2\sigma_1^+ = \sigma_2/L$ . For  $N = 1000$ , we obtain the results presented in figure 9(b).

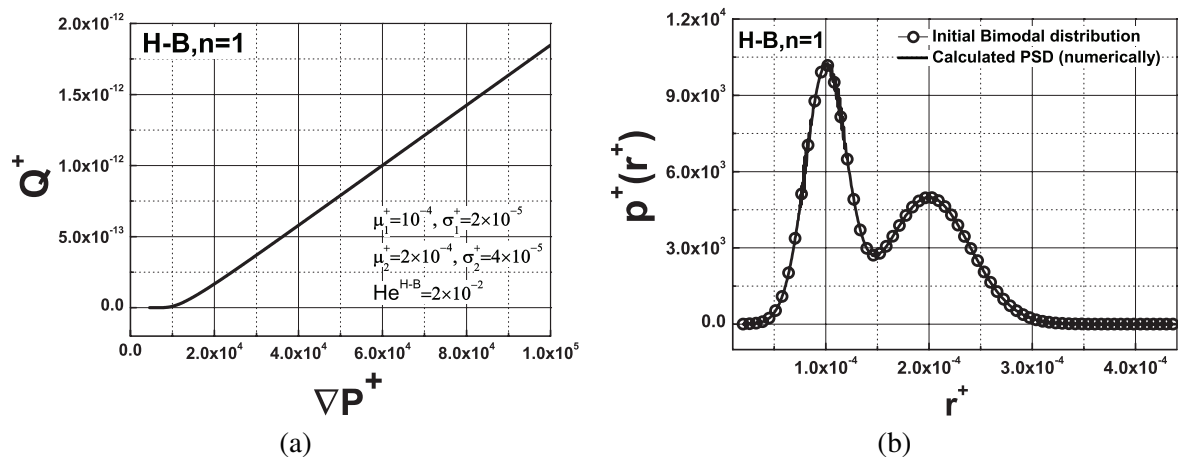


FIGURE 9: (a) Total flow rate vs. pressure gradient for a bimodal distribution with  $\mu_2^+ = 2\mu_1^+$ ,  $\sigma_2^+ = 2\sigma_1^+$  and a Bingham fluid ( $N = 1000$ ) (b) Comparison between the initial and the numerical method calculated PSD for a bimodal distribution with  $\mu_2^+ = 2\mu_1^+$ ,  $\sigma_2^+ = 2\sigma_1^+$  and a Bingham fluid ( $N = 1000$ ).

#### — Herschel-Bulkley fluid (with $n = 0.9$ and $n = 1.2$ )

Let us remember that this case required the use of non-integer derivatives and showed fluctuations related to the necessary fit (see Fig. 6(b)). Using the same previous procedure, we get the following results (Fig. 10(b) and Fig. 11(b)) for  $n = 0.9$  and  $n = 1.2$ , and for a tri-modal distribution with  $\mu_2^+ = 2\mu_1^+$ ,  $\mu_3^+ = 3\mu_1^+$  and  $\sigma_2^+ = 3\sigma_1^+/2$ ,  $\sigma_3^+ = 2\sigma_1^+$ .

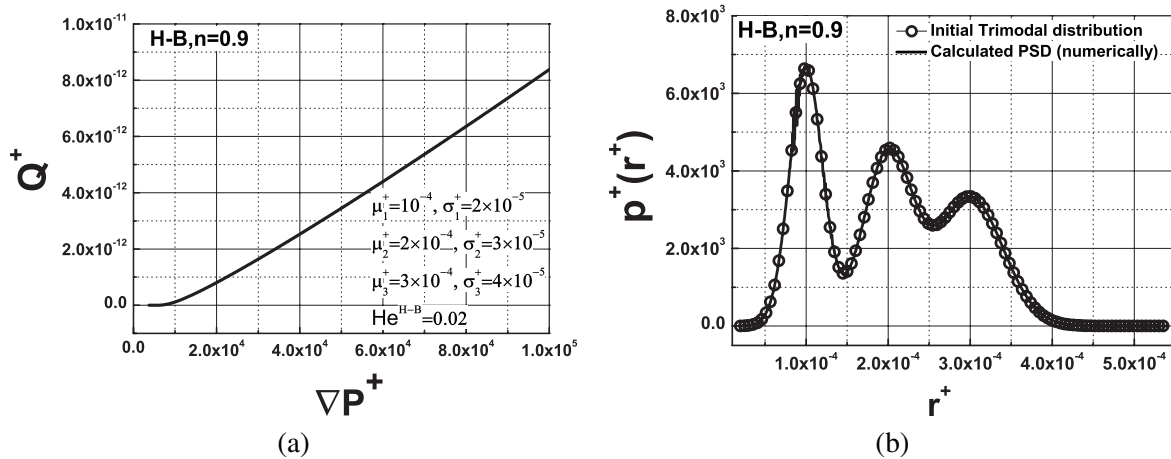


FIGURE 10: (a) Total flow rate vs. pressure gradient for a tri-modal distribution with  $\mu_2^+ = 2\mu_1^+$ ,  $\mu_3^+ = 3\mu_1^+$  and  $\sigma_2^+ = 3\sigma_1^+/2$ ,  $\sigma_3^+ = 2\sigma_1^+$  and a Herschel-Bulkley fluid ( $n = 0.9$ ) (b) Comparison between the initial and the numerical calculated PSD for a tri-modal distribution with  $\mu_2^+ = 2\mu_1^+$ ,  $\mu_3^+ = 3\mu_1^+$  and  $\sigma_2^+ = 3\sigma_1^+/2$ ,  $\sigma_3^+ = 2\sigma_1^+$  and a Herschel-Bulkley fluid ( $n = 0.9$ ).

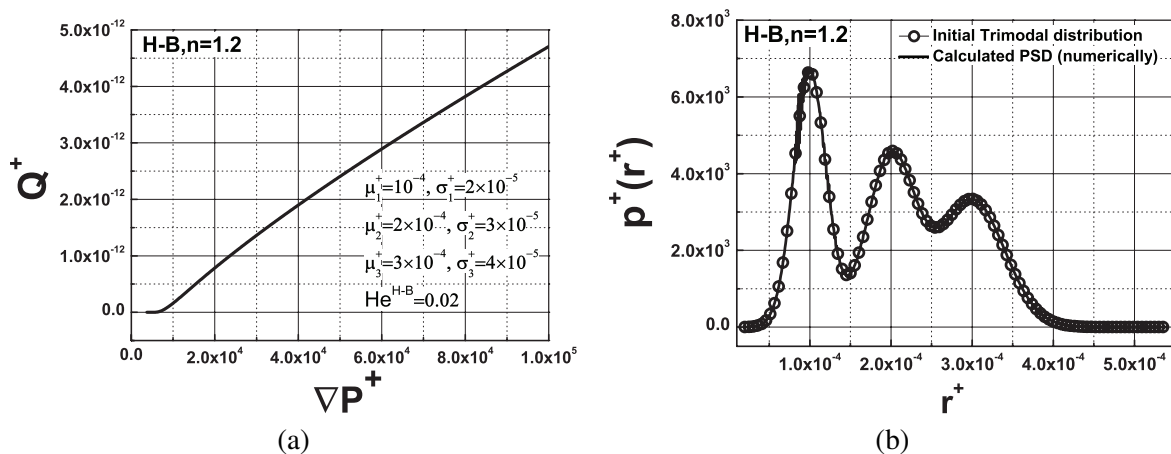


FIGURE 11: (a) Total flow rate vs. pressure gradient for a tri-modal distribution with  $\mu_2^+ = 2\mu_1^+$ ,  $\mu_3^+ = 3\mu_1^+$  and  $\sigma_2^+ = 3\sigma_1^+/2$ ,  $\sigma_3^+ = 2\sigma_1^+$  and a Herschel-Bulkley fluid ( $n = 1.2$ ) (b) Comparison between the initial and the numerical calculated PSD for a tri-modal distribution with  $\mu_2^+ = 2\mu_1^+$ ,  $\mu_3^+ = 3\mu_1^+$  and  $\sigma_2^+ = 3\sigma_1^+/2$ ,  $\sigma_3^+ = 2\sigma_1^+$  and a Herschel-Bulkley fluid ( $n = 1.2$ ).

Once again, this numerical method is therefore effective and robust and can be applied to all yield stress fluids such as the Herschel–Bulkley for any power-law index  $n < 1$  (pseudoplastic behavior) or  $n > 1$  (dilatant behavior) and for all kinds of distributions.

All these tests show that the numerical inversion method is relevant for determining the pore size distribution  $p(r)$  provided that a sufficient number of points and well-adapted radius and pressure gradient intervals are taken. We have been able to reverse the problem of identifying the pore size distribution by a method based on a numerical analysis using a Herschel-Bulkley fluid. The effectiveness of this numerical approach has been proven by applying it to different Gaussian pore size distributions.

### 3 Conclusion

This work presents a new method for determining and identifying the pore size distribution of porous materials. It is based on the capillary bundle model like most of the alternative experimental techniques. This method is based on the existence of a yield stress in non-Newtonian fluids. This threshold gives the possibility of scanning the pore distribution and leads to a Volterra integral equation of the first kind whose kernel is analytically known. The mathematical determination of the probability density  $p(r)$  function is made possible by using the partial derivatives of the total flow of fluid through the porous medium as a function of the pressure gradient. This technique is successfully tested for Herschel-Bulkley type fluids (realistic model) in the case of mono, bi or tri-modal Gaussian distributions, any other distribution or other yield stress fluid (Robertson-Stiff type) could be used, nevertheless the resolution of the Volterra equation in some cases should be done numerically and not analytically. Finally, this method could so become in the future as an alternative, non-toxic and cheap method for the characterization of porous materials.

### Références

- [1] F. A. L. Dullien, Porous media - Fluid transport and pore structure, Academic Press 2nd ed. (1992).
- [2] A. E. Scheidegger, The physics of flow through porous media, University of Toronto Press 3rd ed. (1974).
- [3] M. Kaviany, Principles of heat transfert in porous media, Springer 2nd ed. (1995).
- [4] P. M. Adler, Porous media : geometry and transports, Butterworth-Heinemann (1992).
- [5] Z. E. Heinemann, Fluid flow in porous media, Textbook series 1 (2003).
- [6] E. P. Barrett, L. G. Joyner and P. P. Halenda, The determination of pore volume and area distributions in porous substances. Computations from Nitrogen isotherms, J. of Am. Chem. Soc. 73 (1951) 373-380.
- [7] M. Brun, A. Lallemand, J-F Quinson and C. Eyraud, A new method for the simultaneous determination of the size and the shape of pores : the thermoporometry, Thermochim. Acta 21 (1977) 59-88.
- [8] H. Tamon and H. Ishizaka, Saxe study on gelation process in preparation of resorcinol-formaldehyde aerogel, J. of Colloid and Interface Science 206 (1998) 577-582.
- [9] D. Pearson and A. J. Allen, A study of ultrafine porosity in hydrated cements using small angle neutron scattering, J. of Material Science 20 (1985) 303-315.
- [10] A. I. Sagidullin and I. Furo, Pore size distribution in small samples and with nanoliter volume resolution by NMR cryoporometry, Langmuir 24 (2008) 4470-4472.
- [11] J. M. Haynes, Stereological analysis of pore structure, J. Materials and Structures, 6 (1973) 175-179.
- [12] A. Oukhlef, S. Champmartin and A. Ambari, Yield stress fluids method to determine the pore size distribution of a porous medium, J. of Non-Newtonian Fluid Mechanics, 204 (2014) 87-93.
- [13] A. Oukhlef, Détermination de la distribution de tailles de pores d'un milieu poreux, Thèse de doctorat, ENSAM d'Angers, 2011.

- [14] J. Kozeny, Über kapillare leitung des wassers im boden, Stizungsberichte der Akademie der Wissenschaften in Wien 136(2a) (1927) 106-271.
- [15] P. C. Carman, Fluid flow through granular beds, Trans. Inst. Chem. Engin. 15 (1937) 154-155.
- [16] W. R. Purcell, Capillary pressure - Their measurement using mercury and the calculation of permeability therefrom, J. Petr. Tech., 1 (1949) 39-48.
- [17] R. B. Bird, R. C. Armstrong and O. Hassager, Dynamics of polymeric liquids, 2nd ed., vol. I, New York : Johon Wiley and Sons, (1987).
- [18] A. Ambari, M. Benhamou, S. Roux and E. Guyon, Pore size distribution in a porous medium obtained by a non-Newtonian fluid flow characteristic, C. R. Acad. Sci. Paris, t. 311, série II (1990) 1291-1295.
- [19] M. R. Malin, Turbulent pipe flow of Herschel-Bulkley fluids, Int. Comm. Heat Mass Transfer, 25 No. 3 (1998), 321-330.
- [20] K. B. Oldham and J. Spanier, The fractional calculus, Academic Press, (1974), p. 53.